INVESTIGATING CENTRAL PIT FORMATION MECHANISMS USING INFERENTIAL STATISTICS, AN UPDATE. S. E. Peel[1] and D. M. Burr[1], [1]Department of Earth and Planetary Sciences, The University of Tennessee, Knoxville (speel1@vols.utk.edu).

Introduction: Central pit craters (CPCs) are complex craters that contain centrally located, approximately circular depressions on crater floors (floor pits) and on central peaks (summit pits) that are formed during crater emplacement [Fig. 1; e.g., 1-3] and are found on many solid bodies across the solar system [e.g., 3-9]. Given the breadth of conditions (i.e. target properties, gravity) that must allow for central pit formation on this wide range of host bodies, the requirements for central pit formation are not well understood.

Many formation mechanisms for central pits have previously been proposed (Table 1) for the CPCs of Mars and elsewhere and have been investigated using methods such as crater inventories and descriptive statistics, morphological analyses, and modeling [e.g., 10, 3, 11-13]. We are testing the previously proposed formation mechanisms for Mars central pits using inferential statistical analyses based on relationships that should be present for each formation mechanism (Table 2). A discussion of the statistical setup and power analyses conducted for this project are included in [14]. The statistical test structure is summarized in Table 3. Because floor and summit type central pits may be formed by different mechanisms, the analyses for each mechanism are conducted separately.

Hypothesis	Sources
(A) Explosive release of volatiles from the subsurface	[15-18]
(B) Collapse of a central peak	[19-21]
(C) Subsurface drainage of water melt	[22]

Table 1: Previously proposed hypotheses tested here.

Hyp	(Test) Relationship
(A, C)	(1) CPCs should have a higher occurrence of volatile-rich ejecta than non-CPCs. [23]
(A)	(2) The volume of the central pits should be greater than the volume of their rims. [24]
(B)	(3) The diameters of central pit rims should be wider than the diameters of central peaks. [24]

Table 2: The relationships that have been proposed to support one or more of the proposed hypotheses.

Data Collection: We independently assessed the global impact crater database of [25] in order to derive a robust population of CPCs for our statistical analyses. Where the Context Camera (CTX) imagery [26] did not enable confident determine of whether the CPC was a floor or summit type pit, HRSC [27-28] digital elevation models (DEMs) and MOLA pedr points [29] were used to take profiles across the crater floor to make this determination (Fig. 1). Where HRSC and MOLA coverage did not have the necessary spatial resolution to resolve the central pit floor (relative) elevation the crater was removed from the population.

To prevent our results from being affected by processes unrelated to central pit formation, we looked at these complex craters in CTX imagery using Google Earth [30] and JMars [31] and determined if they had sufficient preservation, limited infilling, and were not elongated. A detailed discussion of the methodology we are using to determine feature diameters and volumes is included in [14]. Crater ejecta morphology was determined using CTX and THEMIS [32] imagery in GoogleEarth and JMars. Crater diameter measurements are done in JMars. All crater volume measurements are being conducted in ArcGIS [33] using CTX DEMs made with NASA's Ames Stereo Pipeline [34]. The results to date are summarized in Table 3.

Discussion of Assumptions: Based on current models of lobate ejecta emplacement, we identify whether lobate ejecta is present around a sampled crater regardless of where it occurs stratigraphically within a (layered) ejecta sequence. Under the interpretation that lobate ejecta signify the presence of volatiles in the target materials at the time of formation [e.g., 35], this approach identifies CPCs that formed in volatile-rich target materials.

Based on feedback from participants in the 2017 Lunar and Planetary Science Conference concerning assumptions about volatile deposit depths inherent in our testing, we are currently considering altering the ejecta test so that we base our analysis only on the style of ejecta deposit that is present atop any other ejecta deposits present (lobate or radial). This possible change in methodology is based on our understanding that, largely, the ejecta nearest the crater and emplaced last is sourced predominantly from the greatest depth in the target (Fig. 2; [36]), and therefore closest to the material that forms the central pit. We would like to request feedback from the participants of the Planetary Crater Consortium about the accuracy of the above ejecta emplacement model as it pertains to our testing: ***Is the uppermost ejecta within the continuous ejecta blanket predominantly comprised of material excavated from the greatest depth in the target?***

References: [1] Smith, E. I. (1976) *Icarus 28*, 543-550. [2] Hale, W. S., Head, J. W. (1981) *LPI 441*, 104-106. [3] Barlow, N. G. (2010) *GSA Sp. Papers 465*, 15-27. [4] Croft, S. K. (1983) *JGR: Solid Earth (1978-2012) 88.S01:* B71-B89. [5] Moore, J. M., Malin, M. C. (1988) *GRL 15*, 3, 225-228. [6] Schenk, P. M. (1993) *JGR 98*, E4, 7475-7498. [7] Xiao, Z., Komatsu, G. (2013) *Planet. and Sp. Sci. 82-83*, 62-78. [8] Xiao, Z., et al. (2014) *Icarus 227*, 195-201. [9] Russell, C. T. (2015) *DPS 47*, abs. #201.01. [10] Barlow, N. G. (2006) *Met. and Planet. Sci. 41*, 1425-1436. [11] Senft, L. E., Stewart, S. T. (2011) *Icarus 214*, 67-81. [12] Elder, C. M., et al. (2012) *Icarus 221*, 831-843. [13] Barlow, N. G. (2015) *GSA Sp. Paper 518*, 1-34. [14] Peel, S. E., Burr, D. M. (2017) LPSC 48, abs. #1020. [15] Hodges, C. A. (1978) *LPS 9*, 521-522. [16] Hodges, C. A. (1978) *NASA Tech. Mem. 79729*, 169-171. [17] Wood, C. A., et al. (1978) *LPSC 9*, 3691-3709. [18] Wood, C. A., et al. (1978) *Rep. Planet. Geol. Prog. 1977-1978*, 166-168. [19] Greeley, R. et al. (1982) *Sat. of Jupiter*, 340-378. [20] Passey, Q. R., Shoemaker, E. M. (1982) *Sat. of Jupiter*, 379-434. [21] Schenk, P. M. (1993) *JGR 98*, E4, 7475-7498. [22] Croft, S. K. (1981) *LPISC 12*, 196-198. [23] Barlow, N. G. (2009) *LPSC 40*, abs. #1915. [24] Bray, V. J., et al. (2012) *Icarus 217*, 115-129. [25] Robbins, S. J., Hynek, B. M. (2012) *JGR 117*, Res. 117, E06001. [26] Malin, M. C. et al. (2007) *JGR: Planets (1991-2012), 112(E5)*. [27] Neukum, G., et al. (2004) Mars Express: The scientific payload, 17-35. [28] Jaumann, R., et al. (2007) Pl. and Space Sci. 55, 928-952. [29] Smith, D. E., et al. (2001) Geophys. Res. 106, 23689-23722. [30] Google Inc. (2009), v. 7.1.7.2600 [Software] www.google.com/earth/. [31] Christensen, P.R. et al. (2009) abs. #IN22A-06. [32] Edwards, C. S., et al. (2011) JGR 116, E10008. [33] ESRI (2011) ArcGIS Desktop: Resease 10.1. Redlands, CA: Environmental Systems Research Institute. [34] Moratto, Z. M. et al. (2010) *Proc. LPS XLI*, abs. #2364 [35] Carr, M. H., et al. (1977) JGR, 82(28), 4055-4065. [36] Melosh, H. J., (1989) *Impact Cratering: A Geologic Process.* [37] Sheskin, D. J. (2004) *Handbook of Parametric and Nonparametric Statistical Procedures.*

Test	Stats Test [37]	H_o	H_{alt}	Results
(1)	Chi-square test for homogeneity	Total occurrence of volatile-rich ejecta for CPCs ≤ total occurrence volatile-rich ejecta for non-CPC complex craters	The total occurrence of volatile-rich ejecta for CPCs > the total occurrence of volatile-rich ejecta for non-CPC complex craters	Could not reject H_o: p_{fl}=0.44; p_{sum}=0.48
(2)	T-test for two dependent samples	Mean volume of the pit rim ≥ mean volume of the pit	Mean volume of the pit rim < mean volume of the pit	(This test is ongoing)
(3)	T-test for two independent samples	Mean central pit rim diameter ≤ mean central peak diameter	Mean central pit diameter rim > mean central peak diameter	(This test is ongoing)

Table 3: Statistical tests and their null and alternate hypotheses with results [14].

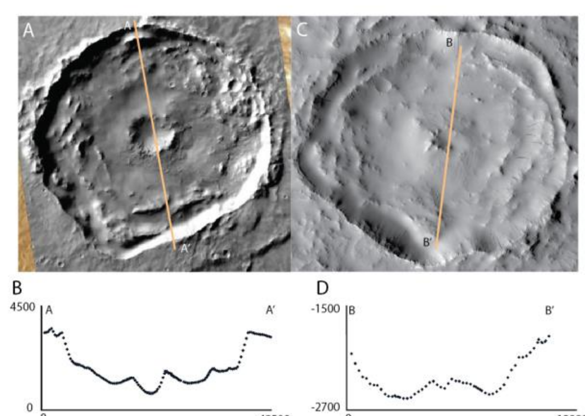

Fig. 1: Floor (A, B) and summit (C, D) CPCs showing morphology (A, C) and relative elevations of the floors (B, D) of the central pits as shown in MOLA PEDR data.

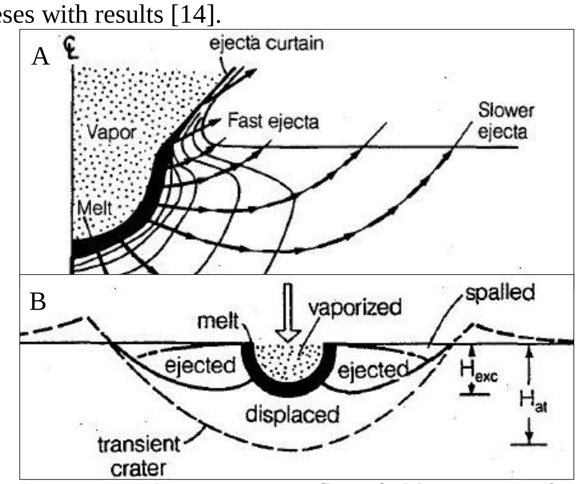

Fig. 2: (A) The excavation flow field geometry from figure 5.9 in [36]. Material higher within each ejecta "streamtube" ejects at a greater velocity than deeper material. (B) From [36], figure 5.13, showing the initial position of ejected and displaced material.